

© 2023 IEEE. Personal use of this material is permitted. Permission from IEEE must be obtained for all other uses, in any current or future media, including reprinting/republishing this material for advertising or promotional purposes, creating new collective works, for resale or redistribution to servers or lists, or reuse of any copyrighted component of this work in other works.

BEV Energy Consumption Estimation for Route Planning

Zdeněk Mašek

Faculty of Transport Engineering, Department of Electrical and
Electronic Engineering and Signalling in Transport (KEEZ)
University of Pardubice
Pardubice, Czech Republic
zdenek.masek@upce.cz

Michal Závodník

Faculty of Transport Engineering, Department of Electrical and
Electronic Engineering and Signalling in Transport (KEEZ)
University of Pardubice
Pardubice, Czech Republic
michal.zavodnik@student.upce.cz

Abstract— The issue of battery electric vehicles (BEVs) is a hot topic in 2023, and one that has a lot of crossover beyond academia. Although BEVs are significantly more energy efficient than vehicles with conventional internal combustion engines [1], the operational range of EV is still considered as one of the main limitations of this technology. Because of this, BEVs need to be able to estimate as accurately as possible the energy consumption of driving and the associated operational range limitation. This paper focuses on the design of an algorithm for detailed simulation of BEV driving in order to determine the total power consumption for typical routes in Central European conditions. The paper presents the BEV driving simulation algorithm and simulation results for typical routes. Furthermore, a comparison of the simulation results with data measured in real world driving of a BEV in real traffic is made. The results show that the total energy consumption of the journey can be estimated before the start of the journey using the presented algorithm with a standard mean deviation of up to 10%. The presented algorithm can serve as one of the determining elements of a comprehensive solution for finding the most suitable driving route and adds the energy aspect of route selection optimization to existing algorithms.

Keywords—battery electric vehicle (BEV), simulation, route planning, energy consumption

I. INTRODUCTION

Personal electromobility is becoming an everyday reality within the EU. This is evidenced by statistics that show a year-on-year increase in sales of pure battery electric vehicles (BEVs) from 3% in 2019 to 12.1% in 2022 [2] of all personal vehicles sold within the EU. In the Czech Republic, there has been an increase [3] from 0.3% in 2019 to 2.03% in 2022, with current data for the pending year 2023 indicating further growth (2.5% at the end of February 2023). Overall, there are already hundreds of thousands of pure electric vehicles whose range is limited by the total capacity of the traction battery.

In the literature, one can come across experimentally oriented papers dedicated to determine the real BEV consumption (e.g. [1][4]). The data clearly shows that the consumption of these vehicles changes significantly with the type of travelled route. Not only the average speed of the vehicle and the remaining capacity of the traction battery [5][6], but also the average slope of the route and the possibility to use recuperated energy, have a major impact on the operating range of the BEV. To illustrate, an example [1] can be given, where under Czech conditions, the BEV Hyundai Kona Electric 64 kWh achieved a consumption of 14.1 kWh/100 km in urban traffic and 21.7 kWh/100 km in highway operation. This resulted in a reduction of the

vehicle's operational range from 454 km (urban) to only 295 km (highway). From this example it is clear that for algorithms that calculate the operational range (remaining achievable driving distance), it is not sufficient to consider only current or previous data, i.e. to statistically process data from the last few tens of kilometres of BEV driving. When calculating the achievability of the driving destination, it is also appropriate to consider the parameters of the route sections that are yet to be driven. It is therefore the ability to faithfully model the energy consumption of the BEV on the particular link of the road.

In terms of the design of the algorithm for calculating the energy consumption of a route, we can talk about so-called online and offline algorithms. Online algorithms are used in vehicle control units, where they are used to calculate the actual, i.e. immediate, operational range of the vehicle. The algorithms are based on past and current data from the BEV sensors. In contrast, offline algorithms are primarily used outside the vehicle and are used to simulate the complete vehicle journey. Thus, the purpose is to determine the BEV consumption on a specific route before the start of the journey. There are a number of approaches to the simulation itself. When designing the algorithm, it is necessary to consider how thoroughly the vehicle will be simulated. Whether to assume only vehicle driving resistances, or also consider non-traction consumption [6], recuperation, or the effect of traction battery aging). Similarly, it is necessary to consider how thoroughly the route will be simulated. Whether to consider only the length, slope and speed limit or also the current/predicted traffic or ambient temperature [7][8], and so on. However, all of these simulation parameters must be included with respect to the target application, as an overly detailed simulation may be disproportionately demanding on computational power.

This paper is devoted to the design of an offline algorithm that is not only capable of predicting the vehicle consumption on a given route, but is also compute-light. This can be considered a necessity if the offline algorithm should not only be used to calculate an already given route, but should also serve as a route optimization tool within the navigation system. The algorithm considers also recuperated energy and non-traction energy consumption of the vehicle. The advantage of the presented algorithm is the calculation of the energy consumption in each sub-section of the route. This makes the algorithm very easy to identify the most energy-intensive sections of the selected route for subsequent route optimization or determination of the real range area.

II. SIMULATION ALGORITHM

This paper describes an algorithm for calculating the energy consumed by a vehicle for traversing a route. The algorithm was developed to be used in a web application to find the ideal route from point A to point B with use of a map-based data. The route is searched based on several factors, where each factor has a certain weight. One of the factors is the energy consumed to traverse the route. The routing algorithm tries to minimize the cost function by selecting appropriate route links. Knowing the state of charge of the electric vehicle battery at the beginning of the route, it is possible to calculate the remaining energy in the battery at the end of the route or to calculate and display the range area of the vehicle on a map [9]. The vehicle characteristics (vehicle drag, vehicle weight, traction and regenerative drive efficiency, power consumption of auxiliary appliances - 12 V on-board network and HVAC) and the characteristics of the individual route links (speed limit, elevation, number of stops) are taken into account. The application does not communicate with the vehicle in any way. The necessary vehicle characteristics would either be entered by the user or read from the database.

A. BEV model

The vehicle model is used to calculate the power consumed from the traction battery. The battery power is contributed by the power at the wheel P_{wh} and the power consumption of the auxiliary appliances P_{aux} (12 V on-board supply and HVAC), which does not depend on the vehicle speed. For both, the efficiency with which the power is consumed from the battery is taken into account.

Power of traction battery when $P_{wh} > 0$ (BEV in drive):

$$P_{bat} = \frac{P_{wh}}{\eta_{dis}} + \frac{P_{aux}}{\eta_{aux,move}} \quad (1)$$

Power of traction battery when $P_{wh} < 0$ (recuperation):

$$P_{bat} = P_{wh} \cdot \eta_{chg} + \frac{P_{aux}}{\eta_{aux,move}} \quad (2)$$

Power of traction battery when $P_{wh} = 0$ (BEV standstill):

$$P_{bat} = \frac{P_{aux}}{\eta_{aux,idle}} \quad (3)$$

The efficiency of the powertrain when recuperating η_{chg} includes the degree of recuperation, which depends on the specific vehicle. The efficiencies $\eta_{aux,move}$ and $\eta_{aux,idle}$ are described in Table I. Two η_{aux} efficiencies are used because of their different values especially in the case of ICE (model can be used for both BEVs and ICEs). The power at the wheels P_{wh} is determined from the vehicle's driving resistance, the resistance from acceleration, the resistance from the slope of the section travelled and the vehicle's instant speed.

$$F_{wh} = A \cdot \cos(\theta) + B \cdot v + C \cdot v^2 + m \cdot d \cdot a(v) + m \cdot g \cdot \sin(\theta) \quad (4)$$

$$P_{wh} = F_{wh} \cdot v / 3.6 \quad (5)$$

Where F_w is the force at the wheels in N , P_{wh} is the power at the wheels in W , v is the speed in km/h , θ is the angle of incline of the track in $degrees$, and a is the acceleration in m/s^2 . The meaning of the other quantities is given in Table I. Acceleration $a(v)$ is read from the table as a function of the average speed of the phase of the link travelled (see subsection C for details).

The vehicle model can be used not only for an electric vehicle but also for an internal combustion engine vehicle. For a conventional internal combustion engine vehicle, the vehicle parameters shall be set to other efficiencies and zero recuperation efficiency.

For the vehicle model, it is most important to enter the following parameters correctly (the number of asterisks indicates the importance):

- Traction drive efficiencies η_{dis} and η_{chg} ****.
- Vehicle drag coefficients A, B, C **.
- Total vehicle mass m **.
- P_{aux} * - has the greatest effect on routes with low average speeds (e.g. in urban areas).

TABLE I. VEHICLE MODEL PARAMETERS

Parameter	Unit	Meaning
m	kg	Total vehicle mass.
P_{aux}	W	Average power consumption of auxiliary drives (12 V on-board supply + HVAC).
η_{dis}	-	Average efficiency of the traction drive when consuming energy from the battery.
η_{chg}	-	Average efficiency of energy recuperation from the traction drive back to the battery. It includes a vehicle-specific rate of recuperation.
$\eta_{aux,idle}$	-	The average efficiency with which power is consumed from the traction battery for auxiliary drives when the vehicle is at standstill.
$\eta_{aux,move}$	-	The average efficiency with which power is consumed from the traction battery for auxiliary drives when the vehicle is moving.
A	N	Vehicle driving resistance coefficients.
B	N/km/h	
C	N/(km/h) ²	
d	-	Rotating mass coefficient.
v_tbl	km/h	Array of speeds at the boundaries of intervals in which vehicle acceleration values are defined.
a_pos_tbl	m/s ²	Array of average positive accelerations of the vehicle in each speed interval v_tbl . It is used when the vehicle is accelerating.
a_neg_tbl	m/s ²	Array of average negative accelerations of the vehicle in each speed interval v_tbl . It is used when the vehicle is braking.

B. Route model

The route consists of individual links. The number of links depends on the specific route. For example, one particular country route of distance 113 km has 906 links. Each link is described by its parameters, which are included in the map data (Table II). The maps are static and do not consider actual traffic or traffic lights.

The basic parameters of each route link are:

- Link length.
- Average slope.
- Permissible speed.

It is also necessary to determine whether the vehicle will stop at the end of the link (typically when crossing from a minor road to a major road, approach to a roundabout or traffic lights) and for how long. A parameter *Cross* has been added to the link description, which assigns to each link a four-level verbal probability of the vehicle stopping at the end of the link (no stop, small, medium, large stop probability). Each verbal value of the stop probability is assigned a specific numerical probability (in the range 0 to 1) and a stopping time in seconds in the algorithm for calculating the energy consumption of the link. For each verbal probability value, the algorithm contains a stop counter and a stop request counter. The fraction of which is used to calculate the interim stop probability separately for each verbal value of the *Cross* parameter. See Table III. If the interim stop probability is lower than the required stop probability, the vehicle will be stopped at the end of the link. If the continuous probability is greater than or equal to the required one, no stop shall be made at the end of the link.

Not only the stop probabilities are different for each value of the parameter *Cross*, but also a difference is made between driving in the urban area and outside the urban area. The *Urban* parameter is used to toggle the desired stopping probability and stopping times at the end of the section for urban and non-urban driving. The stopping probability values were determined by comparing the number of stops in the simulation with the number of stops in the real journeys against which the simulation was validated.

The stopping times were set according to the average length of stops in real journeys in and out of urban areas. It is likely that the probabilities and stopping times will be different on routes other than those on which the test runs took place. The probabilities and stopping times can be tailored e.g. according to the actual traffic density of the link travelled. However, the relationship between probabilities and stopping times and traffic density needs to be established in some way, but this was not part of this project. If the vehicle is travelling on the highway (detection via the *FC* parameter), the stopping at the end of the section according to the *Cross* parameter is disabled.

TABLE II. BASIC PARAMETERS OF EACH ROUTE LINK

Parameter	Unit	Meaning
<i>link_length</i>	m	Length of the link.
θ	deg	Average slope of the roadway in the link.
v_{max}	km/h	Max. permissible speed in the link.
$v_{max,next}$	km/h	Max. permissible speed in the following link.
<i>Cross</i>	-	The verbal probability of stopping at the end of the link. It can take 4 values: <i>not stopping</i> , <i>small</i> , <i>medium</i> , <i>large</i> .
<i>FC</i>	-	Functional categorization of roads. From highways to secondary roads.
<i>Urban</i>	-	Whether or not the link lies within a urban area.
<i>tgt_stop_prob_urban_tbl</i> <i>tgt_stop_prob_country_tbl</i>	-	Array of three required numerical probabilities of a vehicle stopping at the end of a link in the urban area and outside the urban area. Allocated to each value of the parameter <i>Cross</i> .
<i>stop_time_urban_tbl</i> <i>stop_time_country_tbl</i>	s	A field of three vehicle stopping times at the end of the link in the urban area and outside the urban area. Allocated to each value of the parameter <i>Cross</i> .

TABLE III. AUXILIARY PARAMETERS OF EACH ROUTE LINK

Parameter	Unit	Meaning
<i>stop_req_cntr_urban_tbl</i> <i>stop_req_cntr_country_tbl</i>	-	Array of three stop request counters at the end of the links in the urban area and outside the urban area. For each value of the parameter <i>Cross</i> . Incremented in the link each time the <i>Cross</i> parameter requests a stop.
<i>stop_cntr_urban_tbl</i> <i>stop_cntr_country_tbl</i>	-	Array of three stop counters at the end of the links in the urban area and outside the urban area. For each value of the parameter <i>Cross</i> . It is incremented each time a vehicle actually stops at the end of a link.
<i>act_stop_prob_urban_tbl</i> <i>act_stop_prob_country_tbl</i>	-	An array of three continuously calculated numerical probabilities of stopping at the end of a link in the urban area and outside the urban area. For each value of the parameter <i>Cross</i> .

C. Calculation of energy consumption in the link

The calculation of the energy consumption of an electric vehicle is based on the simulation of a model vehicle driving along a defined route. The route consists of links, where each link is described by its parameters. The basis is the calculating of the energy consumed in the link. The total energy E_{trip} consumed along the route is obtained by summing the energies in the links $dE_{link}(k)$, equation (6).

$$E_{trip} = \sum_{k=1}^n dE_{link}(k) \quad (6)$$

Important requirements were the simplicity and speed of the calculations and the ability to calculate energy consumption on a link-by-link basis, without knowledge of the entire route before running the calculations. The presented algorithm for calculating the energy consumed does not need to have the whole route defined in front. At each moment it is sufficient to know only the given link and, if available, the allowed speed from the next link. If the allowed speed from the next link could not be obtained (because the next link is not known), the algorithm can manage without it. The allowed speed from the next link is only used for the "braking before the speed limit sign" function, the absence of which hardly affects the resulting energy. The allowed speed, defined in each link of the route, enters the calculation as the desired speed. The vehicle tries to maintain this allowed speed by accelerating, decelerating or driving at a constant speed. The calculated speed at the end of the link is fed into the calculation of the following link, where it is used as the initial speed at which the vehicle entered the link. The counters used to calculate the probability of stopping at the end of the link are also passed between the link calculations. The data transfer between links is illustrated in Fig. 1. The algorithm for calculating the energy consumption of a link can be used without modification for both an electric vehicle and a conventional vehicle with an internal combustion engine.

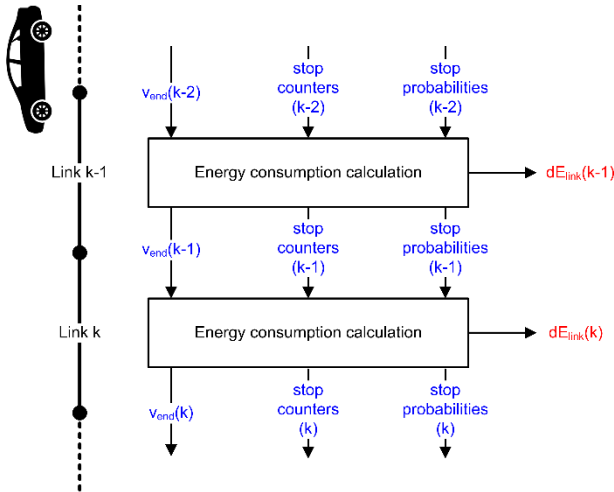


Fig. 1. Data flow in the calculation of energy consumed in the section

Each link is divided into 4 phases:

- Phase 1 - initial dynamical phase
- Phase 2 - constant speed phase
- Phase 3 - final dynamic phase
- Phase 4 - standstill phase at the end of the link

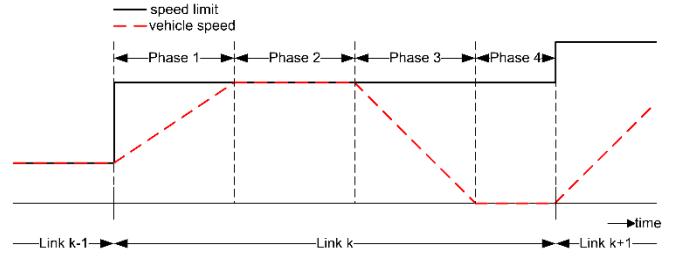


Fig. 2. Dividing the link into phases

The splitting of the link into the above 4 phases covers all possible ways of vehicle passage through the link. Not all phases need always be represented in the link. Which of them will be used in the calculation depends on the vehicle's travel through the particular link. For example, if the vehicle does not stop at the end of the link and the speed limit is the same or higher in the following link, the end dynamic phase (phase 3) and the standstill phase (phase 4) are eliminated.

In each phase the following parameters are calculated:

- distance travelled
- driving time (or standstill time)
- average speed in phase
- instant speed at the end of the phase
- energy consumed

Simple formulas describing driving at constant speed and acceleration are used in vehicle motion calculations. This speeds up the calculations significantly. Acceleration is used as a constant in the dynamic phases. Based on the initial and final speeds in the dynamic phase, the table a_{pos_tbl} or a_{neg_tbl} is used to read out the corresponding acceleration values at each speed interval from initial to final speed. From these accelerations, the average $a_x(k)$ is calculated and then used in a given dynamic phase x . The table of velocity intervals and the corresponding tables of positive and negative acceleration are included in the vehicle parameters. The acceleration values used in the tables come from real driving of the EV on different types of roads (urban, non-urban, mountain, highway). The initial speed at which the vehicle entered the dynamic phase is the speed at the end of the previous phase. In the initial dynamic phase (phase 1) this is the speed at the end of the previous link. In the final dynamic phase (phase 3) this is the speed at the end of the constant speed phase (phase 2). The end speed in the final dynamic phase (phase 3) is either the maximum speed allowed in the current link, or zero speed if the vehicle is to stop at the end of the link, or the allowed speed from the next link if this is lower than the allowed speed in the current link. From the known acceleration, mean vehicle speed and vehicle parameters, the vehicle driving resistance (power at the wheels) is calculated in each phase. The mean vehicle speed $v_{avg,x}(k)$ is the average speed in the phase. In the constant speed driving phase it is equal to this speed. In the dynamic phase it is not calculated as a normal average, but as a weighted average of the initial and final speeds in that phase, where the higher speed has a weight of 0.75 and the lower speed has a weight of 0.25. This averaging was implemented in order to reduce the error in the calculation of the driving resistances, whose dependence on speed is non-linear (4).

The input variables for the calculation of the vehicle driving resistances (4), (5) are:

- Total vehicle weight m .
- Vehicle driving resistance coefficients A , B , C and dimensionless coefficient of rotating masses d .
- Average v_{avg} speed in phase.
- Average acceleration at phase.
- Average slope in a given link θ .

The battery power P_{bat} in each phase is calculated from the power on the wheels P_{wh} , the known power of the auxiliary P_{aux} drives (12 V supply and HVAC) and their efficiencies. The energy consumed dE in the phase is calculated from the calculated time duration of a given phase and the battery power P_{bat} . Summing the energy consumed in all 4 phases gives the energy consumed in the link $dE_{link}(k)$, where k is the order number of the link.

D. Example of calculation

Assume a vehicle passes through link k according to Fig. 3. The figure shows that the section is long enough to accommodate all phases. This assumption is handled in the example.

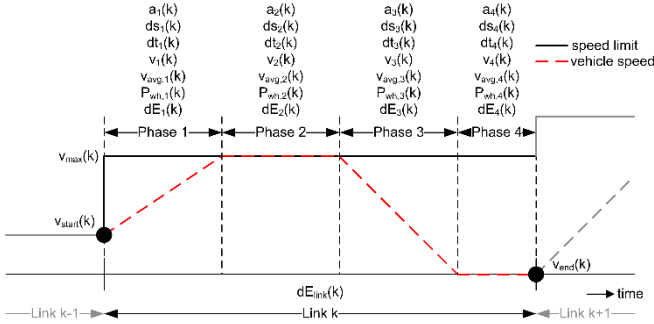


Fig. 3. Vehicle travel through the link

$$v_{start}(k) = v_{end}(k-1) \quad (7)$$

$$v_{end}(k) = 0 \quad (8)$$

If the vehicle would not stop at the end of the link and the speed limit in the next link would be the same or higher than in the current link, the following applies:

$$v_{end}(k) = v_{max}(k) \quad (9)$$

If the vehicle does not stop at the end of the link and the speed limit in the next link is lower than in the current link, the vehicle must brake and then the following applies:

$$v_{end}(k) = v_{max}(k+1) \quad (10)$$

If the speed information from the next link is not available, the vehicle enters the next link at an unreduced speed and starts braking only after entering the next link, equation 9 applies.

Phase 1:

Constant average acceleration in phase 1:

$$a_1(k) = \text{mean}(a_{pos_tbl}(v_{start}(k):v_{max}(k))) \quad (11)$$

Distance travelled in phase 1:

$$ds_1(k) = \frac{v_{max}^2(k) - v_{start}^2(k)}{2 \cdot a_1(k)} \quad (12)$$

Time duration of the phase 1:

$$dt_1(k) = \frac{v_{max}(k) - v_{start}(k)}{2 \cdot a_1(k)} \quad (13)$$

Speed at the end of the phase 1:

$$v_1(k) = v_{max}(k) \quad (14)$$

Average speed at the end of the phase 1:

$$v_{avg,1}(k) = 0.25 \cdot v_{start}(k) + 0.75 \cdot v_{max}(k) \quad (15)$$

Phase 2:

$$a_2(k) = 0 \quad (16)$$

$$ds_2(k) = \text{link_length}(k) - ds_1(k) - ds_3(k) \quad (17)$$

$$dt_2(k) = \frac{ds_2(k)}{v_{max}(k)} \quad (18)$$

$$v_2(k) = v_{max}(k) \quad (19)$$

$$v_{avg,2}(k) = v_{max}(k) \quad (20)$$

Phase 3:

$$a_3(k) = \text{mean}(a_{neg_tbl}(v_{max}(k):v_{end}(k))) \quad (21)$$

$$ds_3(k) = \frac{v_{max}^2(k) - v_{end}^2(k)}{2 \cdot a_3(k)} \quad (22)$$

$$dt_3(k) = \frac{v_{max}(k) - v_{end}(k)}{2 \cdot a_3(k)} \quad (23)$$

$$v_3(k) = v_{end}(k) \quad (24)$$

$$v_{avg,3}(k) = 0.25 \cdot v_{end}(k) + 0.75 \cdot v_{max}(k) \quad (25)$$

Phase 4:

$$a_4(k) = 0 \quad (26)$$

$$ds_4(k) = 0 \quad (27)$$

The standstill time at the end of the link depends on the required and continuous stopping probability and on the parameters *Cross*, *Urban*, *FC* (see *Table II*).

We never stop on the highway:

$$\text{if } FC = \text{highway then } dt_4(k) = 0 \quad (28)$$

Off the highway ($FC \neq \text{highway}$):

$$\begin{aligned} &\text{if } act_stop_prob < tgt_stop_prob \\ &\text{then } dt_4(k) = stop_time \\ &\text{else } dt_4(k) = 0 \end{aligned} \quad (29)$$

When driving in the urban area ($Urban = \text{true}$):

$$\begin{aligned} &tgt_stop_prob = tgt_stop_prob_urban_tbl(Cross) \\ &act_stop_prob = \frac{stop_cntr_urban_tbl(Cross)}{stop_req_cntr_urban_tbl(Cross)} \end{aligned} \quad (30)$$

When driving outside the urban area ($Urban \neq \text{true}$):

$$\begin{aligned} &tgt_stop_prob = tgt_stop_prob_country_tbl(Cross) \\ &act_stop_prob = \frac{stop_cntr_country_tbl(Cross)}{stop_req_cntr_country_tbl(Cross)} \end{aligned} \quad (31)$$

$$v_4(k) = 0 \quad (32)$$

$$v_{avg,4}(k) = 0 \quad (33)$$

The following equations are used in all stages:

$a_x(k)$, $ds_x(k)$, $dt_x(k)$, $v_{avg,x}(k)$.

$$\begin{aligned} F_{wh,x}(k) &= A \cdot \cos(\theta(k)) + B \cdot v_{avg,x}(k) + C \cdot v_{avg,x}^2(k) \\ &+ m \cdot d \cdot a_x(k) + m \cdot g \cdot \sin(\theta(k)) \end{aligned} \quad (34)$$

$$P_{wh,x}(k) = \frac{F_{wh,x}(k) \cdot v_{avg,x}(k)}{3.6} \quad (35)$$

$$dE_x(k) = \left(\frac{P_{wh,x}(k) \cdot dt_x(k)}{\eta_d} + \frac{P_{aux}(k) \cdot dt_x(k)}{\eta_{aux}} \right) \cdot \frac{1}{3600} \quad (36)$$

If $P_{wh,x}(k) \geq 0$ (power consumption from the battery):

$$\eta_d = \eta_{dis} \quad (37)$$

If $P_{wh,x}(k) < 0$ (recuperation):

$$\eta_d = \frac{1}{\eta_{chg}} \quad (38)$$

If $v_{avg,x}(k) > 0$:

$$\eta_{aux} = \eta_{aux,move} \quad (39)$$

If $v_{avg,x}(k) = 0$:

$$\eta_{aux} = \eta_{aux,idle} \quad (40)$$

Where x is the phase number (1, 2, 3, 4) and k is the sequence number of the link.

The energy to drive the vehicle through the link:

$$dE_{link}(k) = \sum_{x=1}^4 dE_x(k) \quad (41)$$

Given example is simplified. In practice, the length of the individual phases must be checked against the length of the link. Some phases may be dropped. Therefore, the dynamic phases are calculated first. If the link is too short for the vehicle to stop, the deceleration applied is adjusted to a value that ensures that the vehicle stops at the end of the link. This does not correspond to reality, but apparently it cannot be done otherwise. It is not possible to start braking several links ahead, because the whole route is not known in advance. In the case of a speed reduction only at the end of the link, braking is handled in the same way.

III. RESULTS ACHIEVED

The energy consumed for the route calculated by the presented algorithm was compared with real trips of a Hyundai Kona electric 64 kWh car with heat pump in summer (ambient temperature 13 to 32 °C). In total, 23 runs were performed on different types of routes in the Czechia [1]:

- urban area of city Pardubice (1 route, 6 trips)
- county roads (2 routes, 4+4 trips) - eastern and central Bohemia
- mountains - Deštné in Orlické hory mountains (1 route, 4 trips)
- highway D11 (1 route, 5 trips – max. speed 2x 90 km/h and 3x 130 km/h)

The length of the routes varies from 77 to 124 km. It is therefore a mix of different types of routes with different total vehicle weight, slope, level of use of air conditioning, weather, traffic density and with two different drivers.

A. Vehicle model settings

The total vehicle mass m was set separately for each simulation run according to the actual vehicle mass in that run (from 1810 to 2082 kg depending on vehicle occupancy).

The powertrain efficiencies were set to the average values obtained from the analyses of the real runs of used vehicle ($\eta_{dis} = 0,92$, $\eta_{chg} = 0,63$). Both efficiencies of power draw from the traction battery to the auxiliary drives ($\eta_{aux,move}$ and $\eta_{aux,idle}$) were set to 0.9.

The power consumption of the P_{aux} auxiliary drives was set equally in all driving simulations to a constant average value of 520 W based on analyses of real driving.

Vehicle driving resistances A , B , C were set according to the EPA database [13]. The coefficient of rotating masses $d = 1.1$. The values of the average accelerations during acceleration (a_{pos_tbl}) and braking (a_{neg_tbl}) were set based on the analyses of real trips [1]. There is a total of 13 speed intervals from 0 to 130 km/h.

B. Setting up the route model

The description of each route was provided by an external company in shape format.

The stopping probabilities at the end of the link $tgt_stop_prob_urban_tbl$ and $tgt_stop_prob_country_tbl$ for the 3 values of the parameter *Cross* (small, medium, large stopping probability) were determined by comparing the number of stops in the simulation with the number of stops in the real runs. So as to achieve the best possible match in the number of stops in the city and outside the city. They take values between 0.05 and 0.5. The stopping probabilities are the same for all route links and for all simulated routes. The stopping times have been set according to the average stopping time in real trips in and out of urban areas and are the same for all simulated routes.

C. Results

Simulations were performed in Matlab.

A total of 23 simulations were performed and compared against 23 real trips. Table IV and Table V show the results of the simulated trips, which were grouped by route type and averaged. A positive error in % means that the value of the variable in the simulation is larger than in reality. Table VI shows the statistical parameters of the error in the calculation of the energy consumed on each route type. Table VII shows the statistical parameters of the whole dataset of 23 simulations. Fig. 4 shows the histogram of the errors of the consumed energy calculation of this dataset. A normal probability distribution of the data set was considered.

TABLE IV. AVERAGE RESULTS FROM SIMULATED RUNS ON INDIVIDUAL ROUTE TYPES

	highway	mountain	country road	urban area
Total mass [kg]	1866	1946	1903	1810
Distance travelled [km]	82,0	93,0	93,4	82,9
Travel time [hh:mm:ss]	0:47:36	1:52:39	1:34:26	2:35:56
Average speed [km/h]	108,0	49,4	59,4	31,9
Number of stops on the route	5	28	56	154
Vehicle standstill time [s]	109	588	1171	3234
Specific consumption energy [kWh/100km]	18,6	13,7	14,3	13,7
Consumed energy [kWh]	15,0	12,7	13,0	9,1

TABLE V. COMPARISON OF SELECTED VARIABLES BETWEEN SIMULATION AND REALITY ON INDIVIDUAL ROUTE TYPES

	highway	mountain	country road	urban area
Distance travelled error [%]	0	0	-2	-4
Travel time error [%]	-9	-12	-13	-28
Average speed error [%]	10	14	14	35
Number of stops on the route error [%]	9	157	201	0
Vehicle standstill time error [%]	12	-50	104	-6

Specific energy consum. error [%]	9	-1	18	4
Energy consumed error [%]	9	-1	8	-3

TABLE VI. MAGNITUDE OF THE ERROR IN THE CALC. OF THE ENERGY CONSUMED ON EACH TYPE OF ROUTE

Type of route	Average Error	Standard deviation of error	Range of errors
Highway	+8.6%	6.9%	+3% to +22%
Mountain	-1.3%	0.8%	-1% to -3%
Country road 1	+17.7%	7.6%	+10% to +29%
Country road 2	-1.6%	2.1%	-5% to +0%
Urban area	-3.1%	9.2%	-15% to +13%

TABLE VII. STATISTICAL MAGNITUDE OF THE ERROR IN THE CALC. OF THE ENERGY CONSUMED IN ALL 23 SIMULATED TRIPS

Average value	3.6%
95% confidence interval of the mean value	-0.9% to +8.1%
Standard deviation	10.4%
For 95% of trips, the error in the calculation of the energy consumed is within the range	-16.8% up to +24.0%

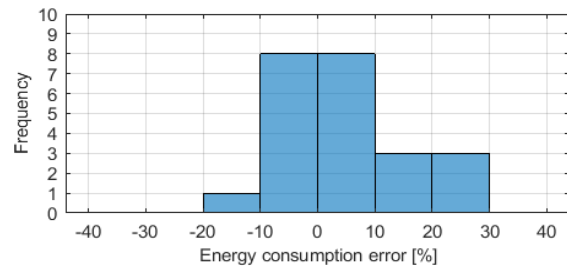


Fig. 4. Energy consumption error histogram of simpler algorithm

D. Effect of air conditioning

The implementation of a unified average power input of the P_{aux} auxiliary drives on all routes caused an increase in total energy consumption in those simulations where the real power input of the auxiliary drives was lower (air conditioning off in real driving). Conversely, in simulations where the real power input of the auxiliary drives was higher (air conditioning on in real driving), the total energy consumption decreased. The differences are larger the lower the average speed on the route (largest differences in the city, smallest on the highway). Table VIII shows 2 trips without air conditioning and 4 trips with air conditioning in the urban area for comparison. The average deviation in energy consumption changes by 15.6% when the air conditioning status is changed. The average difference in energy consumption observed in real city driving trips with air conditioning on and off was about 15%, i.e. identical. On county roads and highway, it was between 3 and 8%.

TABLE VIII. EFFECT OF AC ON DRIVING SIMULATION

	Urban without A/C		Urban with A/C			
Energy consumed deviation [%]	+13	+2	+1	-15	-10	-10
Energy consumed average deviation [%]	+7.3		-8.3			
Energy consumed average deviation [%]						-3.1

IV. MORE COMPLEX ALGORITHM

In addition to the (simpler) algorithm described above, a more complex algorithm has been developed that more faithfully describes the vehicle's driving on the route. However, it has the following major disadvantages:

- It requires knowledge of the entire route in advance.
- The computation time is about one order of magnitude longer.

The basic principle of the calculation is the same. However, the calculations of the average values of the variables in the individual phases of each section are replaced by the solution of the differential equation of the vehicle motion in equidistant time steps (simulation step 0.1 s). The vehicle motion is thus simulated more faithfully, especially braking to a lower speed for several links ahead. Another major difference between the algorithms is the different way of determining the stopping points along the route. In the more complex algorithm, which was developed first, the stopping probability is not implemented. In the more complex algorithm a vehicle stops whenever a crossing from a minor to a major road is detected in the route link description. The same applies to entering a roundabout. This description is not perfect and, depending on the route, leads to an overestimation or underestimation of the number of stops. The more complex algorithm suffers from a significant underestimation of the number of stops in the urban area and consequent underestimation of energy consumption (Fig. 5, Table IX).

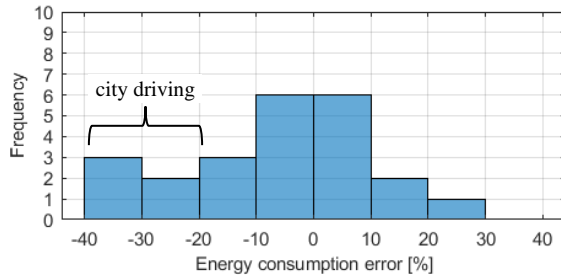


Fig. 5. Energy consumption error histogram of more complex algorithm

V. COMPARISON OF THE RESULTS OF BOTH ALGORITHMS

Table IX shows a direct comparison of the average errors in the calculation of energy consumed between the mentioned algorithms on different types of routes. The largest calculation errors for each route type are marked in red.

TABLE IX. COMPARISON OF ENERGY CALCULATION ERRORS OF BOTH ALGORITHMS ON INDIVIDUAL ROUTE TYPES

	Simple algorithm		Complex algorithm	
	Average Error	Standard deviation of the error	Average Error	Standard deviation of the error
Highway	8.6%	6.9%	7.5%	7.1%
Moutain	-1.3%	0.8%	-5.2%	0.7%
Country road 1	17.7%	7.6%	9.9%	4.7%
Country road 2	-1.6%	2.1%	-7.8%	3.6%
Urban area	-3.1%	9.2%	-28.1%	6.8%

TABLE X. STATISTICAL COMPARISON OF THE ERRORS IN THE CALCULATION OF THE ENERGY CONSUMED BY BOTH ALGORITHMS IN ALL 23 SIMULATED TRIPS

	Simple algorithm	Complex algorithm
Average value	3.6%	-6.2%
95 % confidence interval of the mean value	-0.9% to +8.1%	-13.1% to +0.6%
Standard deviation	10.4%	15.9%
For 95% of trips, the error in the calculation of the energy consumed is within the range	-16.8% to +24.0%	-37.3% to +24.9%

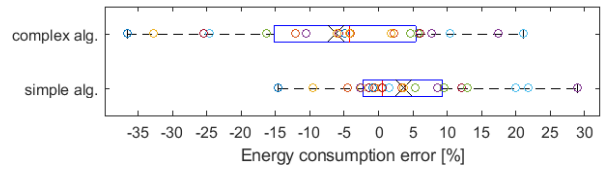


Fig. 6. Statistical parameters of both algorithms on a set of 23 trips

Explanation of the box plot in Fig. 6. The circles are individual trips. The cross indicates the mean value. The red line inside the blue box is the median. The left and right edges of the box are the 25th percentile and 75th percentile. The whiskers represent the minimum and maximum.

VI. EVALUATION OF RESULTS

First, the simpler algorithm will be evaluated. From a practical application point of view, the accuracy of the calculated energy consumption is most important for the evaluation. Therefore, the simulation results were compared with the real measured energy consumption of a Hyundai Kona 64 kWh EV on the same routes (see Table V). The results show that the calculation error depends on the type of route. On highways and county roads, the simulated energy consumption is about 8 to 9% higher than the real one, almost identical in the mountains and about 3% lower than the real one in the urban areas. In all cases, the average vehicle speed in the simulation is higher and the driving time is shorter than in reality. The largest differences (about -30%) are in the urban areas. This is due to the imperfect route description, which does not include information about traffic and other influences that affect the maximum speed at which each link segment can be driven. In the simulation, the vehicle always starts at the maximum speed allowed for the link, which may not be achievable in practice due to the immediate conditions.

The average error in the energy consumption calculation for the set of 23 trips on the 5 route types is +3.6% with a 95% confidence interval of -0.9% to +8.1%. Thus, the average energy consumption is slightly overestimated, with relatively large differences between trips (Table VI, Table VII, Fig. 6). A two-sample paired t-test applied to the dataset of 23 trips did not reject the hypothesis that the mean value of the calculated energy in kWh of the two algorithms coincides with the mean value in the set of real trips (Fig. 7, reality vs. simple alg.).

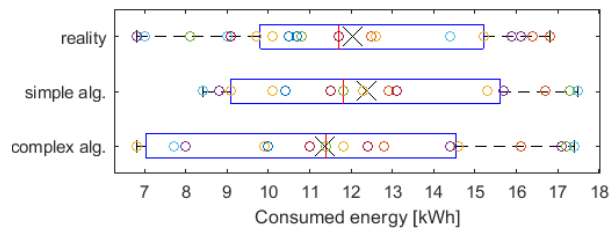


Fig 7. Statistical parameters of the calculated consumption using both algorithms and real trips

In simpler algorithm for 95% of the trips, the error in the calculation of the energy consumed lies between -16.8% and +24.0%. The occurrence of both negative and positive errors in the urban driving simulation is due to the operation of the air conditioning, which is not affected by the simulation because it uses a constant power input from the auxiliary drives. The quantification of the effect of air conditioning on energy consumption has already been done in Section III.D. Another visible difference is between the routes of Country road 1 and Country road 2. Country road 1 runs from the lowlands to the mountains and back (elevation change of 505 m). Country road 2 goes through the lowlands. For the Country road 1 route, the simulation significantly overestimates the energy consumption.

By comparing the results of the more complex algorithm with the simpler algorithm, we find that the more complex algorithm calculates several percent less energy consumption on each type of route than the simpler algorithm. On average, it underestimates the overall energy consumption (see Table X). This is due to the significantly lower energy consumed when driving in the urban area (on average by -28.1%), see Table IX and Fig. 5. The lower calculated consumption is due to an average of 70% fewer vehicle stops in the simulation than in the real runs. This is also related to the approximately 80% increase in average speed and the approximately 50% shorter driving time in the city in the simulation compared to reality. By using a different method of determining stops along the route in a simpler version of the algorithm, the insufficient number of vehicles stops in the urban driving simulation was eliminated. However, the increase in the number of stops in the urban area also affected the non-urban routes. There are too many stops in the simulation compared to the more complex algorithm. Two to three times more than in reality (see Table V). The probability of stopping was set by real routes in the city of Pardubice and clearly does not correspond to passages through small villages on routes outside the urban area.

It can be concluded that the energy consumption calculated in the simulations using the simpler (and faster) algorithm is, with exceptions, in relatively good agreement with reality. It is not significantly worse compared to the more complex algorithm. In city driving, on the other hand, the simpler algorithm performs significantly better.

VII. CONCLUSION

An algorithm for calculating energy consumption on a route constructed from map data was presented. The algorithm's performance was verified on data from 23 real trips of a Hyundai Kona electric 64 kWh MY20 on five different routes in summer. The accuracy of the calculation has a non-negligible variability and depends on the type of route. For 95% of the trips, the error of the energy consumption calculation lies in the range of -16.8% to +24.0%, with a mean error of +3.6%, and a 95% confidence

interval of -0.9% to +8.1%. The accuracy of the calculation depends strongly on the setting of the correct vehicle parameters. The most sensitive parameters in the vehicle model are the efficiencies related to the traction drive. In the route model, it is necessary to find a practical way to determine numerical values for the stopping probabilities at the ends of sections, as this affects the number of stops along the route. The vehicle model parameters in the simulations were set according to the Hyundai Kona electric 64 kWh MY20 vehicle with heat pump. The next stage of development will be to verify the accuracy of the calculation on other types of electric vehicles and in winter season, for which different values of vehicle parameters will have to be found.

The proposed algorithm does not require knowledge of the entire route ahead and is fast to compute. Therefore, it can be used in routing algorithms. The calculated energy in each route link can be part of the evaluation criterion of the routing algorithm. Thus, energy consumption can be considered when finding a suitable route.

REFERENCES

- [1] M. Závodník, Z. Mašek, O. Sadílek, "Selected issues of the energetics of personal electric vehicles", in *Conference ICAI 2022*, ŠKODA AUTO University, 9th–10th June 2022, pp. 226-236.
- [2] ACEA (2022), "Fuel types of new cars 2022" [online]. [cit.2023-02-19]. Available: <https://www.acea.auto/fuel-pc/fuel-types-of-new-cars-battery-electric-12-1-hybrid-22-6-and-petrol-36-4-market-share-full-year-2022/>
- [3] Centrum dopravního výzkumu (2023), "Registrace nových osobních vozidel v ČR" [online]. Čistá Doprava. [cit.2023-02-19]. Available: <https://www.cistadoprava.cz/registrace-novych-osobnich-vozidel-v-cr/>
- [4] De Gennaro, M., Paffumi, E., Martini, G., Manfredi, U., Vianelli, S., Ortenzi, F., Genovese, "Experimental test campaign on a battery electric vehicle: on-road test results (Part 2)". *SAE International Journal of Alternative Powertrains*, vol. 4, iss. 2, pp. 277-292, 2015, doi: <https://doi.org/10.4271/2015-01-1166>.
- [5] Jun Bi, Yongxing Wang, Jiawei Zhang, "A data-based model for driving distance estimation of battery electric logistics vehicles", *EURASIP Journal on Wireless Communications and Networking* 2018, 251 (2018), doi: <https://doi.org/10.1186/s13638-018-1270-7>.
- [6] S. Barcellona, D. D. Simone and S. Grillo, "Real-time electric vehicle range estimation based on a lithium-ion battery model," *2019 International Conference on Clean Electrical Power (ICCEP)*, Otranto, Italy, 2019, pp. 351-357, doi: 10.1109/ICCEP.2019.8890095.
- [7] S. S. Sonaliker and S. D. Shelke, "Estimation of remaining range of electric vehicle using Kalman filter", *2018 International Conference on Inventive Research in Computing Applications (ICIRCA)*, Coimbatore, India, 2018, pp. 632-636, doi: 10.1109/ICIRCA.2018.8596767.
- [8] J. Wang, I. Besselink, H. Nijmeijer, "Battery electric vehicle energy consumption prediction for a trip based on route information", In *Proceedings of the Institution of Mechanical Engineers, Part D: Journal of Automobile Engineering*, 2018, 232(11), pp. 1528-1542.
- [9] Y. Zhang, W. Wang, Y. Kobayashi and K. Shirai, "Remaining driving range estimation of electric vehicle," *2012 IEEE International Electric Vehicle Conference, Greenville, SC, USA, 2012*, pp. 1-7, doi: 10.1109/IEVC.2012.6183172.
- [10] J. Fridlund, O. Wilén, "Parameter guidelines for electric vehicle route planning", Degree project in technology, KTH Royal Institute of Technology, Stockholm, Sweden, 2020.
- [11] J. G. Hayes and G. A. Goodarzi, *Electric powertrain: energy systems, power electronics and drives for hybrid, electric and fuel cell vehicles*, Chichester, UK: John Wiley & Sons, 2018.
- [12] M. Vražić, O. Barić, P. Virtic, "Auxiliary systems consumption in electric vehicle", *Przeglad Elektrotechniczny*, vol. 2014, iss. 12, pp. 172-175. doi:10.12915/pe.2014.12.42
- [13] EPA, "Data on cars used for testing fuel economy", epa.gov, Available: <https://www.epa.gov/system/files/documents/2022-04/21-tstcar-2022-04-15.xlsx> (accessed April 11, 2023)